Large scale simulation of watershed mass transport – a case study of Tsengwen reservoir watershed

Ko-Fei Liu (*Hydrotech Research Institute, National Taiwan University, Taiwan*)
Yi-Chin Chen (*Hydrotech Research Institute, National Taiwan University, Taiwan*)
Ying-Hsin Wu (*Dept. of Civil engineering, National Taiwan University, Taiwan*)

Abstract We present the large scale simulation of watershed mass transport, including landslide, debris-flow and sediment transport. A case study of Tsengwen reservoir watershed under the extreme rainfall triggered by typhoon Morakot is simulated for verification. This approach starts with volume-area relationship formula with inventory method to predict temporal and regional landslide volume production and distribution. Then, debris flow model, Debris-2D, is used to simulate the mass transport of debris-flow from hillslope to fluvial channel. Finally a sediment transport model, NETSTARS, is used for hydraulic and sediment routing in river and reservoir. The integrated simulation for the whole watershed gives a very good agreement with the temporal variation of sediment concentration recorded at the very downstream location.
Keywords. large scale simulation, watershed, Debris-2D, sediment transport, landslide

1. Introduction

Landslide, debris-flow, and sediment transport are often combined phenomenon in the mountainous area, Taiwan is not an exception. When typhoon strikes Taiwan, heavy rainfall triggers high density of landslides in slopeland area. Then the deposit material from landslides is mixed with rainfall or overland flow and becomes debris-flows flowing downstream along hillslope or fluvial channel. Finally, mass from landslides or debris-flows transported into fluvial channel increases river sediment concentration. This chain of mass transport presents multi-hazard potential to human lives, properties and water resource infrastructures. A comprehensive approach to investigate and model this mass transport process has become a critical issue for disaster mitigation and water resources management in Taiwan.

In the past decades, there are many models developed to simulate landslides, debris flows, sediment transport process individually. For landslide, researchers has used empirical or physical models to evaluate the landslide susceptibility (Guzzetti et al., 2005 Chang and Chiang, 2009) and estimate volume of landslides (Khazai and Sitar, 2000; Guzzetti et al., 2009; Klar et al., 2011). For debris-flows, several numerical models such as FLO-2D, RAMMS, and Debris-2D, have been widely used in debris-flow assessment (O'Brien et al. 1993; Liu and Huang 2006, Liu et al., 2012). Especially, Liu et al. (2012) find that Debris-2D can simulate the granular debris flow triggered by landslide very well. In sediment transport studies, various hydraulic models are developed for the simulation of sediment transport such as HEC-RAS, NETSTARS, and CCHE2D (Rathburn and Wohl, 2001; Lee at al., 1997; Lee and Hsieh, 2003; Huang et al., 2006).

However, a comprehensive model for simulating that combined all mass transport processes has not been seen. In this study, we proposed an integrated approach to simulate watershed mass transport process, including landslide, debris-flow, and sediment transport from slopeland to fluvial channel. A case of Tsengwen reservoir watershed under extreme rainfall triggered by typhoon Morakot is used for verification.

2. Methodology

This integrated approach can be separated into three parts - landslide volume estimation and generation, debris-flow simulation, and sediment transport. First, we developed model of landslide volume estimation by mapping landslide inventories and calculated the volume production of individual landslide by volume-area relation. Then, we calibrated the relations between rainfall and landslide volume to construct this temporal and regional volume production model. Second, the output of landslide volume is used as the initiation condition input for the debris flow simulation. A watershed scale simulation for transport of landslide mass by Debris-2D is then performed. Finally, the simulation results of Debris-2D at river junction is used as the sedimentary boundary condition input of NETSTARS to simulate the hydraulic and sediment transport in channel and reservoir. The detailed descriptions for each step are given below:

2.1 Landslide volume model

We collect long term event-based inventory data covered landslides triggered by typhoon events and heavy rainfalls to develop empirical relations between landslide volume and accumulated rainfall. Landslide scars in the inventory were mapped manually by comparing the Formosa-2 and SPOT-4 satellite images taken before and after each event. Then, the volume of individual landslide was estimated by using a volume-area relation as below:

$$V_L = \alpha A_L^{\gamma}, \tag{1}$$

where V_L (unit: m^3) is landslide volume; A_L (m^2) is landslide area; α and γ are calibrated parameters for each small watershed. To link the landslide volume with rainfall, Uchihugi's empirical equation (Uchihugi, 1971) was used for the volume of landslide (Fig. 1):

$$V_L = KA(P - P_0)^r, \tag{2}$$

where K and r is calibrated parameters for watersheds; A is area of watershed; P is cumulative rainfall, and P_0 is a critical rainfall threshold..

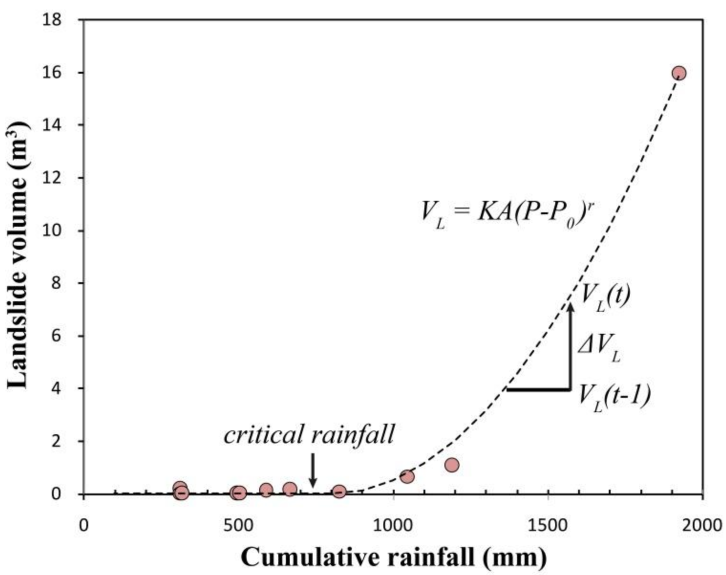

Fig. 1 Schematic relation between landslide volume and cumulative rainfall

Fig. 1 shows the volume change for different cumulative rainfall. Although this curve is obtained from event based data, we can interpret it as the increase of volume in time for increased accumulative rainfall for a landslide. Put it in another word, if this landslide event occurs suddenly and all debris slide down at the same time, we still treat it as if it is produced gradually in time. When the produced volume is small, it can stay in the original location. The mass will slide down only if the cumulative mass is large enough.

With this interpretation, hydrograph of the landslide volume production can be calculated by Eq. (2). Volume production from landslide in a specified time interval can be calculated as

$$\Delta V_L = V_L(t) - V_L(t-1)\,. \tag{3}$$

As for determination of landslide locations, we refer to landslide inventory of the Tsengwen reservoir watershed. Malamud et al. (2004) shows that landslide tends to occur at where it occurred in the past. Besides, shallow landslides usually occur before the peak of rainfall (Godt et al., 2006; Yu et al., 2006), and in the following large ones occur after the rainfall peak (Lollino et al., 2006; Tsou et al., 2010). According to all the literatures, we assumed that old landslide sites tend to be reactivated, and small landslides occurred prior to large ones.

2.2 Debris-flow transport simulation

Being mixed with water from rainfall or overland flow, landslide material on slopeland forms debris flow and transports downstream into the fluvial channel. In this study, this process is simulated by Debrid-2D model (Liu and Huang, 2006). The fundamental theory of Debrid-2D is based on the mass and momentum conservation with shallow water assumption and depth-averaging method. The adopted constitutive relation between shear stress and strain rate is proposed by Julien and Lan (1991). The governing equations are all in conservative forms and the Cartesian coordinates. The mass conservation equation is

$$\frac{\partial H}{\partial t} + \frac{\partial (uH)}{\partial x} + \frac{\partial (vH)}{\partial y} = 0\,, \tag{4}$$

The *x*- and *y*-momentum conservation equations are

$$\frac{\partial (uH)}{\partial t} + \frac{\partial (u^2H)}{\partial x} + \frac{\partial (uvH)}{\partial y} = -gH\cos\theta\frac{\partial B}{\partial x} - gH\cos\theta\frac{\partial H}{\partial x} + gH\sin\theta - \frac{1}{\rho}\frac{\tau_0 u}{\sqrt{u^2+v^2}}\,, \tag{5}$$

$$\frac{\partial (vH)}{\partial t} + \frac{\partial (uvH)}{\partial x} + \frac{\partial (v^2H)}{\partial y} = -gH\cos\theta\frac{\partial B}{\partial y} - gH\cos\theta\frac{\partial H}{\partial y} - \frac{1}{\rho}\frac{\tau_0 v}{\sqrt{u^2+v^2}}\,, \tag{6}$$

where $H = H(x,y,t)$ is debris flow depth; $B = B(x,y)$ is bed topography which assumed to be fixed; *u* and *v* are depth-averaged velocities in x- and y-direction respectively, and they are functions of spatial variables *x*, *y* and temporal variable *t*; tanθ is the average bottom bed slope; ρ is debris-flow density, which is assumed to be constant; *g* is the gravitational acceleration; τ_0 is yield stress, which represents the material property of debris flow. However, due to the fixed bed topography, the erosion effect is not considered during the simulation. In Debris-2D, an initiation condition for any originally stationary debris pile is

$$\left(\frac{\partial B}{\partial x} + \frac{\partial H}{\partial x} - \tan\theta\right)^2 + \left(\frac{\partial B}{\partial y} + \frac{\partial H}{\partial y}\right)^2 > \left(\frac{\tau_0}{\rho g\cos\theta H}\right)^2. \tag{7}$$

Equation (9) means that debris flow can move only if the sum of pressure and gravitational effects, i.e. two terms on LHS, exceeds the yield stress effect, i.e. RHS.

For Debris-2D simulation, the main input is debris flow mass volume distribution. The input of mass volume *V*, is the dry debris volume V_d obtained by the landslide volume model divided by the equilibrium volume concentration C_v (%) of debris flow (Takahashi, 1981)

$$C_v = \frac{\rho\tan\theta}{(\sigma-\rho)(\tan\phi - \tan\theta)}\,, \tag{8}$$

where ρ_w is water density; σ is the density of dry debris (around 2.65 g/cm^3); ϕ is internal friction angle (about 37^o) ; θ is average bottom slope angle in the field.

With the total debris flow volume *V* and the distribution obtained by the landslide volume model and a yield stress measured from the field or estimated with similar soil composition, we can simulate the transport of all landslide volume.

From the simulated result of DEBRIS-2D, we can obtain the locations that debris flow flows into creeks and the corresponding volumes for sediment. Then, these inputs in space and time are used for sediment transport simulation side inflows in rivers.

2.3 Sediment transport

To model sediment transport process in creek and reservoir, we used NETSTARS (Network Sediment Transport Model for Alluvial River Simulation) (Lee et al., 1997). NETSTARS is a quasi-2D numerical model for hydraulic and sediment routing in alluvial channels. The flow in channel can be divided into several stream tubes that all physical properties will be averaged over each stream tube cross-section. For unsteady hydraulic routing, the de Saint Venant equations is used (take flow in *x*-direction for example)

$$\frac{\partial A}{\partial t}+\frac{\partial Q}{\partial x}=0, \tag{9}$$

is the continuity equation, and

$$\frac{\partial Q}{\partial t}+\frac{\partial}{\partial x}\left(\alpha\frac{Q^2}{A}\right)+gA\frac{\partial \eta}{\partial x}+gAS_f-\frac{Q}{A}q=0, \tag{12}$$

is the momentum equation. In Eqs. (11) and (12), A is channel cross-sectional area; Q is flow discharge; q is lateral inflow/outflow discharge per unit length; α is momentum correction coefficient; η is water surface elevation; S_f is friction slope; K is channel conveyance and $K=(A/n)R^{2/3}$ where n and R are Manning's coefficient and hydraulic radius respectively.

Based on the result of hydraulic routing, flow condition in the channel can be obtained and is applied as the input of sediment transport calculation.

As for sediment routing, NETSTARS considers two flow conditions, including equilibrium and non-equilibrium one. If the flow condition is equilibrium, the total transport capacity of sediment load Q_s is calculated by the total load equations as below:

$$\frac{\partial Q_s}{\partial x}+(1-p)\frac{\partial A_{dt}}{\partial t}=0, \tag{10}$$

where A_{dt} is the amount of sediment deposition/scouring per unit length of stream tube; p is bed sedimentary deposit porosity, and $(1-p)$ stands for the volumetric sediment concentration (Julien, 2002). Eq. (13) is also referred to as the 1-D Exner equation.

On the other hand, for non-equilibrium flow condition, the separate treatment method includes three equations, which are the sediment continuity, sediment concentration convection-diffusion equation and bed load equation. The Rouse number is used to separate suspended and bed load. Particle with Rouse number > 5 is treated as bed load, but suspended load if Rouse number ≤ 5. The sediment continuity equation is

$$\frac{\partial Q_b}{\partial x}+(1-p)\frac{\partial A_{dt}}{\partial t}+\frac{\partial}{\partial x}\sum_{k=1}^{N}\left(q_t C_k\right)=0, \tag{11}$$

where Q_b and q_t are bed load transport rate and flow discharge in stream tube respectively; C_k is depth-averaged concentration of suspended sediment of size class k (Holly, 1990). This C_k is calculated using the convection-diffusion equations as

$$\frac{\partial\left(C_k A_t\right)}{\partial t}+\frac{\partial}{\partial x}\left(q_t C_k\right)=\frac{\partial}{\partial x}\left(A_t k_x\frac{\partial C_k}{\partial x}\right)+S_k+\left(hk_z\frac{\partial C_k}{\partial z}\right)_r^l, \tag{12}$$

where k_x and k_z are longitudinal and transverse dispersion coefficients; A_t is stream tube cross sectional area; h is flow depth; S_k is source term of suspended sediment of size fraction k, and it considers the effect of sediment resuspension and deposition. Therefore, the evolution of channel bed can also be assessed during the simulation.

For NETSTARS simulation, there are two categories of input. The first category is topography and channel cross-section data, and the other one is the BCs at the upstream and downstream boundaries. For hydraulic routing, a discharge hydrograph is needed at the upstream boundary, and a rating curve at the downstream boundary. For sediment routing, both the inflow suspended-load concentration and bed-load discharge are required at the upstream boundary. The zero concentration gradient is imposed at the downstream end. The simulation result obtained by Debris-2D is used as lateral mass input in the NETSTARS simulation.

3. Case study – Tsengwen reservoir watershed

3.1 Introduction of the field case

Tsengwen reservoir watershed, with total drainage area of 480 km^2, is located in southwest Taiwan, as is shown in Fig. 2. Elevation ranges from 126 m near the Tsengwen dam (marked as square in Fig.2) to 2,610 m at the upstream boundary which is the Mount Ali (marked as triangular in Fig. 2). There are 15 sub-watersheds. Lithological setting in this watershed is dominated by sandstones and shale with weak rock strength of 10~64 MPa (Taiwan Central Geological Survey, 2012). Based on the data from the Water Resources Agency, Ministry of Economic Affairs of Taiwan (2008), the annual precipitation of Tsengwen reservoir watershed is about 2,800 mm, of which 90% in the wet season (May–September). During this wet season, the main source of precipitation is from typhoons. The heavy rainfall from typhoons usually causes numerous landslides and debris flows in this watershed and brings abundant sediment into the reservoir.

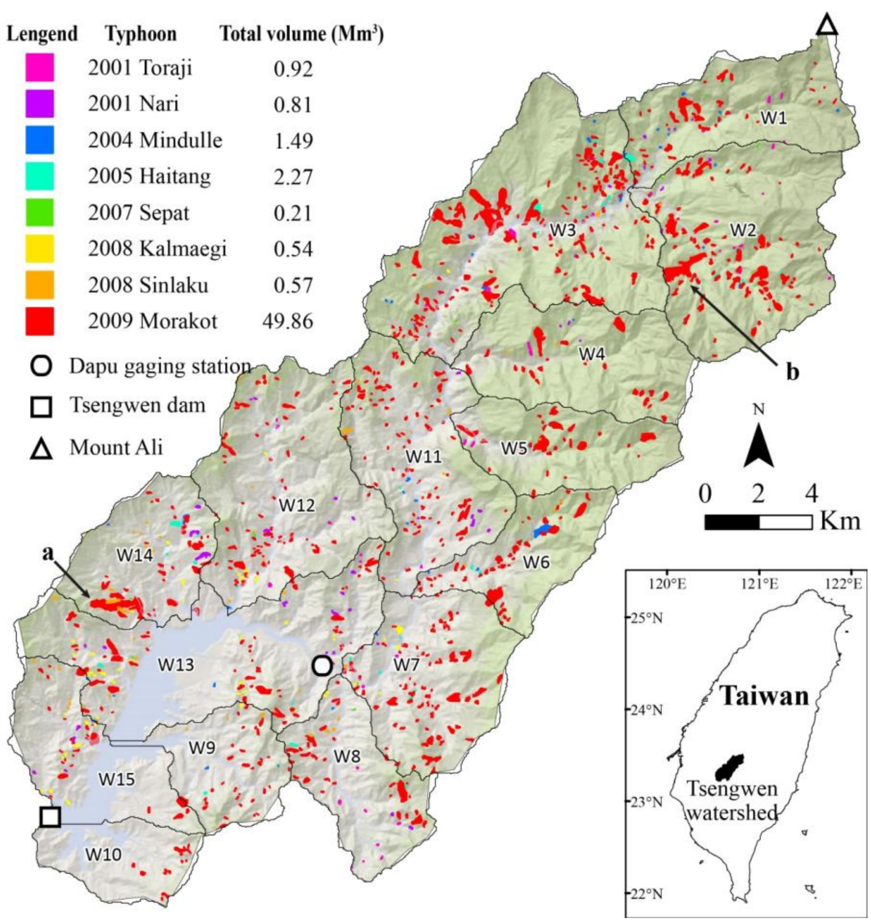

Fig. 2 The distribution of sub-watersheds in the Tsengwen reservoir watershed and landslide inventory of 8 different typhoon events. The landslide locations a and b causes the corresponding peaks a and b in Fig. 3.

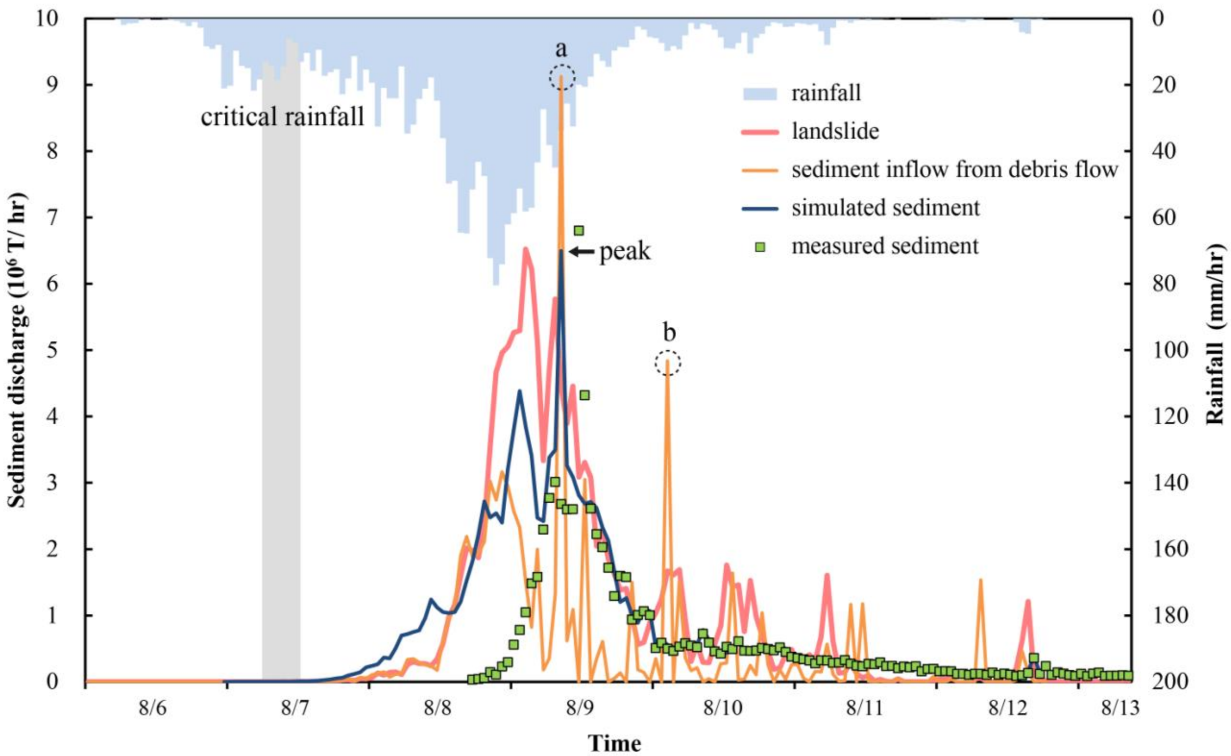

Fig. 3 Hydrograph of rainfall and discharges of simulated landslide volume, channel sediment inflow from debris flow, simulated sediment and measured sediment, which is recorded at Dapu gauging station at downstream. The locations of landslides relating to the peak a and b are marked in the Fig. 2.

Tab. 2 All parameters for landslide volume model, i.e. Eq. (2), and the volumes of landslide and fluvial channel sediment inflow for the 15 sub-watersheds in the Tsengwen reservoir watershed. The ratio of total fluvial channel lateral inflow volume to total landslide volume is 33.9%. RMSE is the abbreviation of root-mean-square error.

watershed ID	A (km^2)	P_0 (mm)	K	r	RMSE (m^3)	Percent error (%)	Landslide Volume (m^3)	Channel Inflow volume (m^3)
W1	28.2	156	0.35	2.7	1.26×105	43	1,970,125	668,087
W2	45.8	156	0.22	2.9	4.65×105	41	8,384,991	3,605,216
W3	64.6	400	0.15	3.0	3.30×105	19	12,428,657	2,950,378
W4	31.3	400	0.32	2.8	7.81×104	25	2,186,534	474,199
W5	22.3	400	3.14	2.6	8.00×104	23	2,497,126	549,704
W6	19.3	159	7.77	2.5	1.95×105	43	2,545,912	853,018
W7	31.8	159	0.94	2.8	2.17×105	53	3,078,364	1,211,712
W8	22.5	159	2.22	2.7	9.20×104	34	1,953,766	369,982
W9	17.5	120	6.28	2.4	2.39×104	30	585,776	155,834
W10	14.7	120	2.73	2.5	1.87×104	37	403,793	86,137
W11	36.7	400	3.27	2.5	6.06×104	25	1,685,969	918,750
W12	45.0	400	1.78	2.6	4.09×104	17	1,636,836	700,049
W13	21.5	805	65.12	2.4	7.26×104	17	2,986,346	1,214,953
W14	23.2	175	0.86	2.9	1.47×105	19	5,264,517	2,136,202
W15	24.7	120	2.43	2.6	3.66×104	18	1,466,701	723,947
						Total	49,075,413	16,618,171

Between August 5 and 10, 2009, typhoon Morakot set a new rainfall record for a single typhoon event in Taiwan. The record is 3,059 mm at the Mount Ali gauging station within the Tsengwen watershed. This extreme rainfall induced large number of landslides and produced a great quantity of sediment. The total sediment volume produced by this single event is the same as the total amount accumulated in the past 19.5 years in the Tsengwen reservoir watershed. (Strong Engineering Consulting Co., 2011)

3.2 Landslide volume

The landslide volumes triggered by the past 8 typhoon events range from 0.21 ± 0.09 to 49.86 ± 6.36 Mm^3. Typhoon Morakot triggered the largest landslide volume in this watershed, accounting for 88% volume of the combined landslide volume from 8 typhoon events. The landslide area and total volume of each typhoon is shown in Fig. 2. From 153 samples, the volume-area relation for the Tsengwen watershed is (Chen et al., 2012),

$$V_L = 0.202 A_L^{1.268}, \tag{13}$$

with the coefficient of determination R^2= 0.78.

All parameters of landslide volume model, i.e. Eq. (2), for the 15 sub-watersheds are shown in Tab. 2. The root mean square errors range from 1.87×10^4 to 4.65×10^5 m^3 and percentage error is between 17% and 53%. The exponent of the model r in Eq. (2), ranging from 2.4 to 3.0, implies that relatively small rainfall increase can result in large increase of landslide volume production. The final output of the total landslide volume in typhoon Morakot is 49,075,413 m^3, and the landslide discharge hydrograph is shown in Fig. 3.

3.3 Debris flow transport simulation

From the debris flow simulation result, the debris flow volume flows into the fluvial channels is used as the lateral sediment inflow discharge. Then this inflow discharge, as shown in Fig. 3, is used as the input of sediment transport simulation. In Fig. 3, there are two peaks of sediment inflow discharge. The first peak comes from the landslide, located at point a in Fig. 2, triggered in the W14 sub-watershed with the volume discharge of 2.46 Mm^3 per hour. The second peak is from the landslide located at point b in the W2 sub-watershed.

The simulated total channel sediment inflow volume from each sub-watershed is listed in Tab. 2. From the simulation result, the total fluvial channel sediment inflow volume from debris flow is about 16,618,171 m^3. So the ratio of sediment input inflow to total landslide volume is about 33.9%, and it is very close to the averaged value 33.3% in Taiwan (value published in the official website of Morakot Post-Disaster Reconstruction Council, 2012).

3.4 Sediment transport

As for NETSTARS simulation, we have to input the cross-sections along the channel and water/sediment inflow at the upstream boundary. Since there is no channel cross section before the disaster, so all channel cross sections are measured after the disaster and it is considered not erodible during the simulation. The input of 240 cross-sections in fluvial channel and reservoir are obtained by digital elevation model (DEM), which is measured by LiDAR with 1 meter resolution and published by WRA (Water Resources Agency).

The water inflow discharge hydrograph at the upstream boundary is determined by area ratio method from transferring the measured discharge hydrograph recorded at Dap gauging station (very downstream, location marked as the hollow circle in Fig. 2).

The sediment rating curve is obtained by the measured datum of the suspended sediment concentrations and the river discharges recorded in Dapu gauging station. The rating curve is shown in Fig. 4,

$$Q_s = 0.6833 Q^{1.9118}, \tag{14}$$

with a goodness of fit R^2 = 0.9421. In this study, we use the water flow discharge with Eq. (17) to obtain the sediment inflow discharge at the upstream boundary.

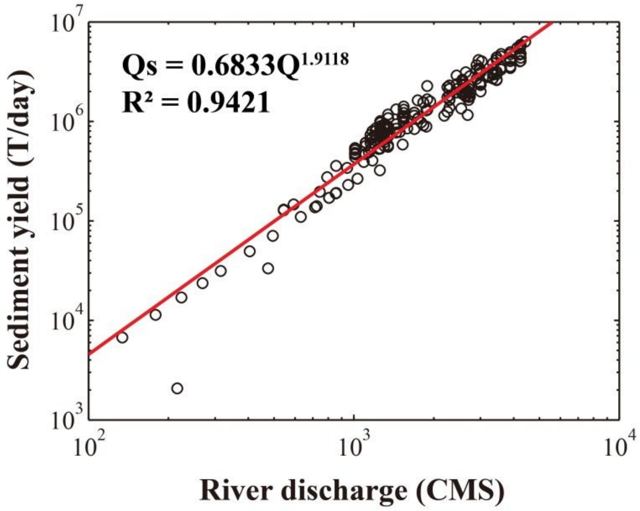

Fig. 4 Sediment rating curve. The unit of sediment yield is Ton per one day. R^2 is the coefficient of determination.

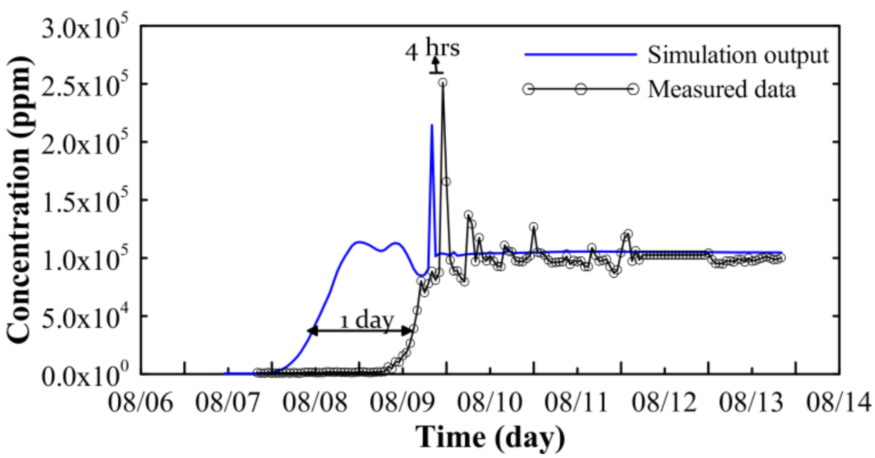

Fig. 5 Comparison of sediment concentration between simulated result and measured data at the Dapu gauging station. The time difference between the simulated and measured peak is 4 hours; and 1 day for the starting time of concentration increase.

To see how good is this large scale simulation method, we use a data that never used in the simulation which is the sediment concentration measured during typhoon at the reservoir dam location. In Fig. 5, the simulation result of sediment discharge is plotted by the blue line, and the sediment discharge measured at the Tsengwen dam is marked by the black circles. When the cumulative rainfall exceeds the critical rainfall (05:00AM~12:00PM on Aug. 7), landslides started to produce mass in all sub-watersheds. The peak of sediment and debris flow discharge happens at the same time, i.e. 8:00 AM on Aug. 9. This peak comes from the large landslide located at point a in Fig. 2 in the W14 sub-watershed. The value of this peak discharge 6.5×10^6 Ton/hr is very close to the measured one, i.e. 6.8×10^6 Ton/hr, which was measured at Dapu gauging station at 11:00 AM on Aug. 9.

However, the simulation result shows that the starting time of concentration increase is one day ahead of the measured data. This is due to the water discharge hydrograph at the upstream boundary. In our simulation, the input discharge is determined by the measured flow discharge at Dapu station in the downstream with the area ratio method. So the upstream hydrograph starts too early. Therefore, the input hydrograph causes the advance of initialization time in the simulation. But those peak concentrations are result of landslides, so the time is

much closer.
The comparison of the simulation and measured sediment concentration of time variation is shown in Fig. 6. The time difference between the two peaks from simulated and measured data is only 4 hours. This is also due to the early start of the assumed input discharge. Although the starting time of concentration increase from simulation is different from the measured one, the tendency of the concentration of time variation is similar. So if input discharge hydrograph is determined by other rainfall-runoff model, such as HEC-HMS, a better simulated result can be obtained.

5. Concluding remarks

We conduct a large scale mass transport simulation including landslide, debris flow and sediment transport in a large watershed. The case of Tsengwen reservoir watershed under the extreme rainfall event triggered by typhoon Morakot is simulation for verification. In the integrated simulation approach, we can obtain the temporal and spatial distribution of landslide volume production with landslide volume model. Then, following the output of landslide model, the debris flow model Debris-2D is used to simulate the mass transport process for the whole watershed. This simulation then provides the lateral mass input into the fluvial channel. Finally, the sediment model, NETSTARS, is used to estimate the time-varying sediment transport concentration in the fluvial channel.
As is verified by the measured sediment discharge at downstream, the simulation result of Tsengwen watershed shows an good agreement of the concentration variation especially in peak amplitude. However, the peak time prediction is early then the real measured data. This is due to the early start of upstream input. A rainfall-runoff model (e.g. HEC-HMS, ANN model, etc.) can provide better time variation even without real measurement from upstream location.
With this comparison, the integrated approach for large scale mass transport simulation seems reasonable and practical and also provides good result. Although early arrival of the peak is not precise, but this result can still be used as warning mechanism where early arrival gives more time for preparation. This approach can also give the sediment information in the fluvial channel and reservoir as the reference for the Tsengwen reservoir operation.

Acknowledgments

The authors would like to thank the Water Resources Agency, Ministry of Economic Affairs of Taiwan for financial support of this research and many valuable and detailed hydrological data.

References

Central Geological Survey, 2012. Surveys of Characteristic of Engineering Rock Masses on hillslopes. (in Chinese) URL: http://envgeo.moeacgs.gov.tw/moeapaper/rock/rock_main.htm
Chang, K.T., Chiang, S.H., 2009. An integrated model for predicting rainfall-induced landslides. Geomorphology 105.3-4, 366-373.
Chen, Y.C., Chang, K.T., Chiu, Y.J., Lau, S.M., Lee, H.Y., 2012. Quantifying rainfall controls on catchment-scale landslide erosion in Taiwan, Earth Surface Processes and Landforms. DOI: 10.1002/esp.3284.
Godt, J. W., Baum, R. L. and Chleborad A. F., 2006. Rainfall characteristics for shallow landsliding in Seattle, Washington, USA. Earth Surface Processes and Landforms 31, 97-110.
Guzzetti, F., Ardizzone, F., Cardinali, M., Rossi, M., Valigi, D., 2009. Landslide volumes and landslide mobilization rates in Umbria, central Italy. Earth and Planetary Science Letters 279.3-4, 222-229.
Holly, F.M., Rahuel, J.-L., 1990. New numerical/physical framework for mobile-bed modeling, Part I: Numerical and physical principles. Journal of Hydraulic Research 28.4, 401-416.
Huang, S.L., Jia, Y.F., Wang, S.S., 2006. Numerical modeling of suspended sediment transport in channel bends. Journal of hydrodynamics 18.4, 411-417.
Julien, P.Y., 2002. River mechanics, Cambridge university press, United Kingdom.
Julien, P.Y., Lan, Y., 1991. Rheology of hyperconcentration. Journal of Hydraulic Engineering ASCE 117.3, 346-353.
Khazai, B., Sitar, N., 2000. Assessment of seismic slope stability using GIS modeling. Annals of GIS 6.2,

121-128.
Klar, A., Aharonov, E., Kalderon-Asael, B., Katz, O., 2011. Analytical and observational relations between landslide volume and surface area. Journal of geophysical research 116.F2, F02001.
Lee, H.Y., Hsieh, H.M., Yang, J.C., Yang, C.T., 1997. Quasi-two-dimensional simulation of scour and deposition in alluvial channels. Journal of Hydraulic engineering ASCE 123.7, 600-609.
Lee, H.Y., Hsieh, H.M., 2003. Numerical Simulations of Scour and Deposition in a Channel Network. International Journal of Sediment Research 18.1, 32-49.
Liu, K.F., Huang, M.C., 2006. Numerical simulation of debris flow with application on hazard area mapping. Computational Geosciences 10, 221-240.
Liu, K.F., Wu, Y.H., Chen, Y.C., 2012. Comparison between FLO-2D and DEBRIS-2D on application of assessment of granular debris flow hazard. submitted.
Lollino, G., Arattano, M., Allasia, P., Giordan, D., 2006. Time response of a landslide to meteorological events. Natural Hazards and Earth System Sciences 6, 179–184.
Malamud, B.D., Turcotte, D.L., Guzzetti, F., Reichenbach, P., 2004. Landslide inventories and their statistical properties. Earth Surface Processes and Landforms 29.6, 687-711.
Morakot Post-Disaster Reconstruction Council, Executive Yuan, Taiwan R.O.C., 2012. (in Chinese) URL: http://88flood.www.gov.tw/eng/
O'Brien, J.S., Julien, P.Y., Fullerton, W.T., 1993. Two-dimensional water flood and mudflood simulation. Journal of hydraulic engineering ASCE 119.2, 244-260.
Rathburn, S.L., Wohl, E.E., 2001. One-dimensional sediment transport modeling of pool recovery along a mountain channel after a reservoir sediment release. Regulated Rivers: Research & Management 17.3, 251-273.
Reichenbach, P., Cardinali, M., Galli, M., Ardizzone, F., 2005. Probabilistic landslide hazard assessment at the basin scale. Geomorphology 72.1, 272-299.
Strong Engineering Consulting Co., 2011 Tsengwen reservoir sedimentation measurements. South Region Water Resources Office, Water Resources Agency, MOEA of Taiwan.
Takahashi, T., 1981. Debris flow. Annual Review of Fluid Mechanics 13, 57-77.
Tsou, C.Y., Feng, Z.Y., Chigira, M., 2011. Catastrophic landslide induced by typhoon Morakot, Shiaolin, Taiwan. Geomorphology 127.3, 166-178.
Uchiogi, T., 1971. Landslides due to one continual rainfall. J.S.E.C.E. 23.4, 79. (in Japanese)
Water Resources Agency, 2008. Hydrological Yearbook of Taiwan Republic of China 2007 Part I - Rainfall. Water Resources Agency, Ministry of Economic Affair of Taiwan.
Yu, F.C., Chen, T.C., Lin, M.L., Chen, C.Y., Yu, W.H., 2006. Landslides and rainfall characteristics analysis in Taipei City during the Typhoon Nari event. Natural Hazards 37, 153–167.

K.F. Liu
Hydrotech Research Institute
National Taiwan University, Taiwan
No.1, Sec. 4, Roosevelt Rd., Taipei 10617, Taiwan
e-mail: kfliu@ntu.edu.tw

Y.C. Chen
Hydrotech Research Institute.
National Taiwan University, Taiwan
No.1, Sec. 4, Roosevelt Rd., Taipei 10617, Taiwan
e-mail: twmtman@gmail.com

Y.H. Wu
Dept. of Civil, Collage of Engineering.
National Taiwan University, Taiwan
No.1, Sec. 4, Roosevelt Rd., Taipei 10617, Taiwan
e-mail: d95521016@ntu.edu.tw